Journal of Volcanology and Geothermal Research 449 (2024) 108064

Contents lists available at ScienceDirect

Journal of Volcanology and Geothermal Research

journal homepage: www.journals.elsevier.com/journal-of-volcanology-and-geothermal-research

SO_2 emission rates and incorporation into the air pollution dispersion forecast during the 2021 eruption of Fagradalsfjall, Iceland

Melissa A. Pfeffer [a,*], Santiago Arellano [b], Sara Barsotti [a], Guðrún Nína Petersen [a], Talfan Barnie [a], Evgenia Ilyinskaya [c], Tryggvi Hjörvar [a,d], Enikö Bali [e], Gro B.M. Pedersen [e], Gunnar B. Guðmundsson [a], Kristín Vogfjörð [a], Eemu Johannes Ranta [e,f], Bergrún Arna Óladóttir [a,e], Brock A. Edwards [g,h], Yves Moussallam [i], Andri Stefánsson [e], Samuel Warren Scott [e], Jean-Francois Smekens [j,k], Matthew Varnam [l,m], Manuel Titos [n]

[a] Icelandic Meteorological Office, Reykjavík, Iceland
[b] Department of Space, Earth and Environment, Chalmers University of Technology, Gothenburg, Sweden
[c] COMET, School of Earth and Environment, University of Leeds, Leeds, United Kingdom
[d] European Centre for Medium-Range Weather Forecasts, IFS section, Bonn, Germany
[e] Nordic Volcanological Center, Institute of Earth Sciences, University of Iceland, Reykjavík, Iceland
[f] Department of Geosciences and Geography, University of Helsinki, Helsinki, Finland
[g] Centre for Earth Observation Science and Department of Environment and Geography, University of Manitoba, Winnipeg, Canada
[h] Geological Survey of Canada, Natural Resources Canada, Ottawa, Canada
[i] Lamont-Doherty Earth Observatory, Columbia University, New York, USA
[j] Department of Earth Sciences, University of Oxford, Oxford, United Kingdom
[k] Department of Astronomy and Planetary Science, Northern Arizona University, Flagstaff, AZ, USA
[l] Department of Earth and Environmental Sciences, University of Manchester, United Kingdom
[m] Lunar and Planetary Laboratory, University of Arizona, Tucson, AZ, USA
[n] Department of Signal Theory, Telematics and Communications, Universidad de Granada, Grenada, Spain

ARTICLE INFO

Keywords:
SO_2
Fagradalsfjall
DOAS
CALPUFF
Volcanic pollution

ABSTRACT

During the low-effusion rate Fagradalsfjall eruption (19 March – 18 September 2021), the emission of sulfur dioxide (SO_2) was frequently measured using ground-based UV spectrometers. The total SO_2 emitted during the entire eruption was 970 ± 540 kt, which is only about 6% of the SO_2 emitted during the similar length Holuhraun eruption (2014–2015). The eruption was divided into five phases based on visual observations, including the number of active vents and the occurrence of lava fountaining. The SO_2 emission rate ranged from 44 ± 19 kg/s in Phase 2 to 85 ± 29 kg/s in Phase 5, with an average of 64 ± 34 kg/s for the entire eruption. There was notable variability in SO_2 on short timescales, with measurements on 11 August 2021 ranging from 17 to 78 kg/s.

SO_2 flux measurements were made using scanning DOAS instruments located at different distances from and orientations relative to the eruption site augmented by traverses. Four hundred and forty-four scan and traverse measurements met quality criteria and were used, along with plume height and meteorological data, to calculate SO_2 fluxes while accounting for wind-related uncertainties.

A tendency for stronger SO_2 flux concurrent with higher amplitude seismic tremor and the occurrence of lava fountaining was observed during Phases 4 and 5 which were characterized by intermittent crater activity including observable effusion of lava and gas release interspersed with long repose times. This tendency was used to refine the calculation of the amount of SO_2 emitted during variably vigorous activity. The continuous seismic tremor time series was used to quantify how long during these eruption phases strong/weak activity was exhibited to improve the calculated SO_2 flux during these Phases.

The total SO_2 emissions derived from field measurements align closely with results obtained by combining melt inclusion and groundmass glass analyses with lava effusion rate measurements (910 ± 230 kt SO_2). Specifically, utilizing the maximum S content found in evolved melt inclusions and the least remaining S content in

* Corresponding author.
E-mail address: melissa@vedur.is (M.A. Pfeffer).

https://doi.org/10.1016/j.jvolgeores.2024.108064
Received 24 November 2023; Received in revised form 15 March 2024; Accepted 25 March 2024
Available online 27 March 2024

accompanying quenched groundmasses provides an identical result between field measurements and the petrological calculations. This suggests that the maximum SO_2 release calculated from petrological estimates should be preferentially used to initialize gas dispersion models for basaltic eruptions when other measurements are lacking.

During the eruption, the CALPUFF dispersion model was used to forecast ground-level exposure to SO_2. The SO_2 emission rates measured by DOAS were used as input for the dispersion model, with updates made when a significant change was measured. A detailed analysis of one mid-distance station over the entire eruption shows that the model performed very well at predicting the presence of volcanic SO_2 when it was measured. However, it frequently predicted the presence of SO_2 that was not measured and the concentrations forecasted had no correlation with the concentrations measured. Various approaches to improve the model forecast were tested, including updating plume height and SO_2 flux source terms based on measurements. These approaches did not unambiguously improve the model performance but suggest that improvements might be achieved in more-polluted conditions.

1. Introduction

An effusive eruption within the Fagradalsfjall volcanic system in Iceland was active from 19 March–18 September 2021 (Barsotti et al., 2023). The six-month long eruption erupted almost exclusively lava, with only very minor tephra, in a mountainous and uninhabited area of the Reykjanes peninsula. The eruption location was, however, within a short distance to critical infrastructure and populated areas at a distance of only about 5 km from the nearest town, 20 km from the international airport in Keflavík, and <50 km from the Reykjavík capital area (Fig. 1).

The volcanic systems of the Reykjanes Peninsula (from west: Reykjanes, Svartsengi, Fagradalsfjall, Krýsuvík, Brennisteinsfjöll) historically erupt in temporal clusters with millennial-scale periods of inactivity (800–1000 years) punctuated by century-scale periods of activity when multiple eruptions from several of the volcanic systems occur (Sæmundsson et al., 2020). The 2021 Fagradalsfjall eruption marks the first eruption on the peninsula in ~800 years (Sigurgeirsson and Sæmundsson, 2022) and we anticipate that there may be more eruptions from Fagradalsfjall or the neighboring systems in the coming months, years or decades. Indeed, there have been two further eruptions in the Fagradalsfjall area as of time of writing: the three-week long Meradalir eruption in August 2022 and the almost four-week long Litli Hrútur eruption in July 2023 as well as three eruptions in December 2023, January 2024 and February 2024 in the neighboring Svartsengi volcanic system. Future eruptions could have greater societal impact if the lava effusion and gas emission rate is higher or if the next eruption site is closer to or within inhabited areas (Óladóttir et al., 2023). This has also come to pass, as the lava flow from the January 2024 eruption destroyed some homes and the lava flow from the February 2024 destroyed essential hot and cold water infrastructure. The long-term hazard considerations for future eruptions in this area include lava flows, air pollution and, in case of an off-shore eruption, tephra fall (Óladóttir et al., 2023).

The 2021 eruption was monitored with continuous and discrete measurements that provided data about ongoing physical and chemical phenomena to forecast the eruptive behavior and to assess and communicate about ongoing hazards (Barsotti et al., 2023). The instrumentation included a seismic network, gas monitoring stations, webcams, automatic weather stations, weather radars, ceilometers, lidars, ground-temperature probes, cGPS stations, and satellite products (Barsotti et al., 2023). Instruments used in this study are indicated in Fig. 1.

Throughout the eruption, the lava effusion rate was quite low (average 9.5 ± 0.2 m^3/s; Pedersen et al., 2022) and the lava posed a relatively limited hazard, constrained spatially within the surrounding valleys (Pedersen et al., 2023). Despite its relatively small size, the eruption caused an increase in ground-level SO_2 concentrations above background levels in most populated areas that were monitored in

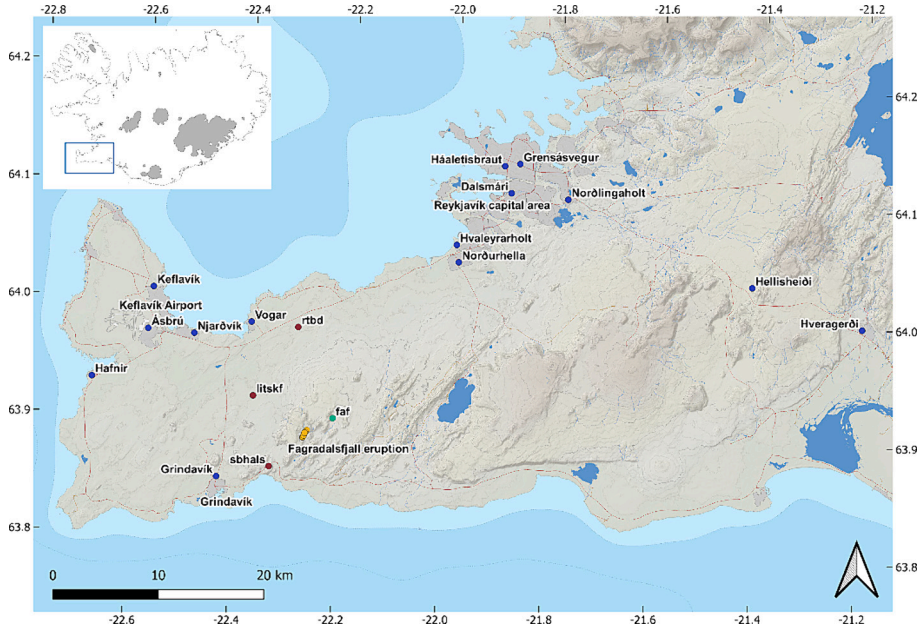

Fig. 1. An overview map showing the locations described in this paper. Eruption vents (yellow), scanning DOASes (red), seismometer (green), EAI SO_2 ground stations (blue), and places with prominent population centers and infrastructure (gray shading). (For interpretation of the references to colour in this figure legend, the reader is referred to the web version of this article.)

Iceland, with maximum distances of 400 km from the eruption site (Whitty et al., 2023). SO_2 can cause adverse health impacts in sensitive individuals (e.g. young and old, asthmatics) even at low concentrations and is therefore monitored in real-time and forecasted prior to and during eruptions. The Icelandic Health Directive air quality (AQ) thresholds for SO_2 (350 μg/m^3 hourly-mean) were exceeded multiple times in populated areas up to ~50 km from the eruption site but most elevations above background were only a few μg/m^3 (Whitty et al., 2023). AQ thresholds were exceeded very frequently at the eruption site (Whitty et al., 2023), which, although uninhabited, attracted over 300,000 visitors during the eruption (Barsotti et al., 2023). (Whitty et al., 2023) will show that the volcanic air pollution fluctuated strongly on very short temporal and small spatial scales. For example, within the densely populated capital area of Reykjavík, the number of SO_2 threshold exceedances varied by up to a factor of 5 between AQ stations located within 1 km of each other, and the hourly-mean SO_2 concentrations could vary by several hundreds μg/m^3 from one hour to the next.

During the eruption, the CALPUFF dispersion model was used to forecast where and when elevated concentrations of volcanic SO_2 could be expected at ground-level (Barsotti et al., 2023). Model results were made available on the website of the Icelandic Meteorological Office twice per day as a 48-h forecast of hourly ground concentration of SO_2. The graphical presentation of the forecast used the colour code system used by the Environmental Agency of Iceland (EAI) to refer to critical SO_2 thresholds of concern for human health (Directorate of Health, 2021). One month into the eruption, two additional maps that showed the most likely areas to be impacted by elevated SO_2 concentrations within 6- and 24-h were also released. Weather forecasters were responsible for daily communication about the ongoing, day-to-day air quality conditions and people were encouraged to check the real-time measurements available on the EAI webpage for gas concentrations at the station closest to them (https://en.vedur.is/volcanoes/fagradalsfjall-eruption/volcanic-gases/ and http://loftgaedi.is). (Whitty et al., 2023) will show that the forecasted ground-level concentrations were often significantly higher than those measured by the EAI measurement network during the Fagradalsfjall eruption.

The CALPUFF model results, as for all volcanic plume dispersion models, are sensitive to the SO_2 flux input parameter which was primarily provided by ground-based SO_2 flux measurements. Differential Optical Absorption Spectroscopy (DOAS) was used as the primary monitoring tool for measuring the emission rate of SO_2 from the eruption. Iceland is a partner in the Network for Observation of Volcanic and Atmospheric Change (NOVAC) consortium (https://novac-community.org) a collaboration between volcano observatories and research institutes to advance monitoring of volcanic emissions. NOVAC-style DOAS measurements, both by scanning the plume from a stationary DOAS (ScanDOAS, (Galle et al., 2010) and traverses with an upward-looking instrument under the plume (MobileDOAS, (Galle et al., 2003) have been successfully applied during the most recent Icelandic eruptions. Frequent DOAS measurements were made during the most recent gas-rich 2014–2015 Holuhraun eruption (Pfeffer et al., 2018) and some DOAS measurements were made during the Eyjafjallajökull 2010 eruption (Donovan et al., 2023; Allard et al., 2011).

The emission rate of SO_2 and other volcanic gases changes in the pre-eruptive phase and over the course of an eruption as the magmatic source changes (such as changing magma composition and crystallinity, e.g. Lerner et al., 2021; Kern et al., 2020), as the environment changes (such as if groundwater is present or not, e.g. De Moor et al., 2016) or as the eruption dynamics are changing (such as physical changes in a lava lake, e.g. Patrick et al., 2016 or changes within the subsurface feeding network, e.g. Scott et al., 2023). Some of the limitations of the gas measurement technique used here are that passive UV remote sensing relies on absorption of diffuse solar radiation (skylight), and therefore can only be done during daylight, which has highly varying length over the course of several months at higher latitudes. Weather conditions impact the quality of the measurements because cloud droplets, aerosols, or haze cause additional scattered light from the surroundings that did not pass through the plume (dilution effect), or differential changes in the effective path lengths of radiation at different wavelengths (multiple scattering effect). These radiative transfer effects may cause severe under- or overestimation of the retrieved gas column densities (e.g. Kern et al., 2010; Varnam et al., 2021; Galle et al., 2023). The uncertainty of the measurements is heavily affected by the uncertainty related to the plume velocity during the measurement. Wind uncertainties can have a large impact on flux retrievals particularly for weak plumes within the atmospheric boundary layer, as general instrumental uncertainty of windspeeds of 1–2 m/s can half/double the calculated fluxes and wind directions become extremely uncertain in weak wind conditions, making it more uncertain which wind speed at which elevation is most suitable. It is thus important to attempt to constrain the uncertainty due to these significant impacts on the determination of the SO_2 flux. Weather conditions in Iceland are very variable. However, most of the time during the six months of the eruption the weather was dominated by southwesterly winds, except in May when northeasterlies dominated (https://www.vedur.is/um-vi/frettir/tidarfar-arsins-2021). The wind speeds during the period, for all months except June, were at or below average. There were a few days with high wind speeds in March and then again in September while the summer was characterized by light winds. In general, the eruption period was characterized by cloudy conditions in SW-Iceland but precipitation was below average. The month of May again deviated from the other months, and it was the sunniest May on record in Reykjavík.

In addition to gas measurements, the SO_2 flux from Icelandic eruptions is also indirectly measured using the petrologic method. This approach utilizes pre-eruptive S concentrations recorded by mineral-hosted glassy melt inclusions, making it possible to constrain SO_2 emissions for eruptions prior to the most recent ones. Such estimates are very useful for initializing dispersal models with an assumed effusion rate prior to an eruption starting or prior to flux measurements being made (Bali et al., 2018; Caracciolo et al., 2023; Devine et al., 1984). This approach relies on an assumption that the SO_2 gas released is directly related to the volume of lava erupted, and that non-erupted magma is not significantly contributing to the gas emissions. With the simultaneous application of direct measurements and the petrologic method to the same eruption, we can now compare and analyze the distinct approaches employed for estimating SO_2 emissions. Furthermore, we can determine the most effective way to incorporate these estimates into real-time dispersion models.

During some eruptions, a relationship has been observed between seismicity and the gas emission rate (Battaglia et al., 2019; Fischer et al., 1994; Hidalgo et al., 2018; Nadeau et al., 2011; Olmos et al., 2008; Salerno et al., 2018). Identifying a relationship between seismicity and gas flux can be extremely helpful as seismic measurements can be continuous, widely distributed, and are not dependent on the same environmental factors and limitations as gas measurements. If a reliable relationship between seismicity and gas emissions is established, it becomes possible to utilize continuous seismic data as an ongoing indicator of concurrent gas flux. However, this relationship relies on the assumption that the physical structures governing the emission of magmatic gases into the air remain relatively stable, at least temporarily.

In this paper we provide the time series of SO_2 emission rates and plume heights measured during the Fagradalsfjall 2021 eruption. We examine variations in measured SO_2 fluxes in relationship to different eruption phases and eruptive behavior and consider the utility of using a continuous time series of seismic tremor as an indicator of the strength of SO_2 release when it is found to be appropriate.

We then use three approaches to estimate SO_2 flux at increasingly high temporal resolution as source terms for an air pollution dispersion model: petrologic (indirect measurements), DOAS (direct measurements), and seismic (continuous proxy). We examine if the

incorporation of these fluxes, as well as incorporation of observations of the volcanic plume height, into the gas dispersion simulations provides more accurate forecasts of ground-level concentrations, thereby enabling improved mitigation of the health harms from eruptive SO_2. We conclude by making recommendations about monitoring gas release rate and forecasting ground-level SO_2 concentration in the build up to and during future Icelandic eruptions.

2. Methods

2.1. DOAS measurements

We used a telescope to collect ultraviolet light from the sun that has been scattered by aerosols and molecules in the atmosphere. Light is collected along a path that intercepts the volcanic plume by scanning or traversing. The light is transferred from the telescope to a grating spectrometer by a quartz optical fiber. In-plume spectra are analyzed against clear-sky and dark spectra and the differential slant column of SO_2 is derived by the DOAS method (Platt and Stulz, 2008). The spectrum range 310–325 or 315–325 and reference files for SO_2, O_3 and ring were used in the retrieval of the slant column amount of SO_2.

Because we used a passive UV-based technique, it can only be used when there is sunlight. The March–September timing of this eruption was very fortunate for acquiring a robust DOAS time series. These measurements were used together with plume height and meteorological conditions to calculate the emission rate of SO_2. We used more sensitive spectrometers with a back-thinned 2D CCD detector (model MayaPro from Ocean Insight) rather than the less sensitive 1D CCD detector more commonly used at lower latitudes (lower signal to noise ratio). We made the measurements in two ways, making traverses beneath the eruption cloud and with continuously operating scanning systems. In total 444 measurements that pass the quality check were made. The quality check includes an overall inspection of the shape of the plume, favoring concentrated plume and completeness of the scan.

2.1.1. DOAS traverses

The eruption occurred in a remote area in localized terms that is only a short distance from the most densely populated region of Iceland. Luckily for making traverse measurements (see for example (Pfeffer et al., 2018) for a description of how traverse measurements are made), the area is surrounded in all directions by paved roads. One hundred and forty-eight traverse measurements were made of which 131 passed the quality check (described below) and were kept. Most of the 131 traverse measurements were made by car with the telescope mounted on the roof of the vehicle. Three of these traverses were made by foot early in the eruption, and four of them were made by a small aircraft in a single day. The SO_2 dispersion forecast (CALPUFF model) was used to determine which road to take and where to start the first traverse in clean air before the plume would be encountered. We made as many repeat traverses as time allowed, on some days making many consecutive repeated traverses to attempt and capture short-term (minutes-hours) changes in flux and on other days we made traverses on the way to/from the eruption site where other work was being done.

The wind data used was mainly upper air meteorological measurements, i.e., balloon-borne radiosonde measurements, made operationally twice a day at Keflavík international airport (18 km from the eruption site), at 00 and 12 UTC, and sometimes supplemented with measurements at 06 and 18 UTC. In addition, short forecasts, 1–12 h, from the operational weather forecast for Iceland, applying the HARMONIE-AROME numerical weather prediction model (Bengtsson et al., 2017) were used to assess if there had been changes in the weather situation and thus the wind regime between the time of the traverse and that of the radiosonde wind measurements.

For a traverse measurement to pass the quality check and be kept in the final dataset, clean air (no detectable SO_2) needed to be measured at the start and end of the traverse (to ensure the entire plume was measured) and there needed to be enough SO_2 within the atmospheric column to be visible in the retrieval. During this eruption, the minimum SO_2 atmospheric column required to have a plume measurable by DOAS traverse was 51 ppm-m.

SO_2 flux was calculated from each traverse measurement using the MobileDOAS software (Johansson, 2009). The software calculates the dominant wind transport direction based on the distribution of SO_2 along the transect and where the maximum SO_2 was detected. The MobileDOAS-indicated dominant wind direction was used to indicate which height of wind data should be used to characterize the main dispersion. The range of altitudes, considering the height of potential existing temperature inversions (as they inhibit vertical transport), that best fit the MobileDOAS-indicated wind direction was used to provide a wind directional sector and upper and lower limits for the wind speed. Four fluxes were calculated from each traverse measurement to provide uncertainty related to meteorological parameters. In cases when the weather regime was varied the estimate had a larger uncertainty than in stable conditions.

2.1.2. DOAS scans

A three-instrument network of scanning DOAS instruments was established as the eruption progressed (10 km NNW of the eruption site, 6 km to the NW and 4.5 km to the SW; red points Fig. 1). Scanning DOAS instruments in Iceland have been adapted to harsh environmental conditions by implementing a non-moving cylindrical quartz window instead of the external rotating hood used at most other locations for the fore-optics of the scanner (Lopez et al., 2017; Pfeffer et al., 2018). Other than this, the instrument is essentially the NOVAC Version I instrument described in Galle et al. (2010) with upgrades to some of the components. These three scanners performed conical scanning with an effective coverage of plumes transported from the eruption site to $\pm 15^\circ$ towards each instrument. For the scanning DOAS measurements, hourly HARMONIE-AROME wind forecasts at 850 hPa (~1400 m a.s.l.) was used in the data selection step and the SO_2 flux calculations. This model wind data indicates that at the height of the plume the wind blew towards the instruments 31% of the time during the eruption. The scanning data was assessed, and fluxes calculated using the NovacProgram software (Galle et al., 2010). We attribute an uncertainty of -50% to $+30\%$ to the scanning DOAS retrievals as described in (Pfeffer et al., 2018), but more recent work (Galle et al., 2023) indicates that this can be an underestimation of the uncertainty, as scattering outside of elevated plumes may have a significant impact on some DOAS measurements.

All scans were examined to determine if they met quality criteria for inclusion. Measurements were excluded from the data set if the wind direction from the eruption to the instrument was greater than $\pm 15^\circ$ of line of sight, if the plume completeness factor assessed by NovacProgram was <0.8 (in a range from 0.5 for a plume seen on the horizon to 1 for a plume with clear sky on both horizons) (Johansson, 2009), if there were full fog conditions at the same time as retrieved column amounts were much higher than measurements close in time but in the absence of fog, and if there were obvious increases in the column amounts during sunrise and sunset. In this eruption, the minimum SO_2 atmospheric column required to have a plume measurable by the DOAS scanners was 16 ppm-m.

Three hundred and thirteen good scan measurements were collected. There were 1609 individual instances when the plume was detected by two instruments simultaneously allowing us to determine the plume height and direction of the plume at those moments. Not all of these instances of two-instrument plume height detections occurred during scans that pass the quality criteria for inclusion in the final SO_2 flux set. This occurs when a partial plume is seen: too little of the plume is seen for inclusion in the flux calculation, but enough of the plume is detected for the wind calculation. Plume heights are additionally included in this study determined from webcam images from Hvassahraun PiCam and Slaga ArduinoCam as reported in (Barnie et al., 2023).

2.2. Eruption phases and seismic tremor

Both (Pedersen et al., 2022; Barsotti et al., 2023) describe the different phases of the eruption based on lava effusion rate and visible characteristics of the eruption. We have applied the same times and descriptions as these papers but have further subdivided the phases based on the intensity of seismic tremor and if the eruption was active or paused (see Table 2 below for details).

The 19-min median of the one-minute average of the 2–4 Hz bandpass-filtered amplitude values of the East component of seismic data from station FAF (green point Fig. 1; 63.9064 N, 22.2148 W), 3.2 km NE of the eruption site (https://doi.org/10.7914/SN/7E_2013) (see Fig. 1) has been used. Prior to applying the median filter, the one-minute bandpass values are multiplied by the gain of the digitizer and divided by the gain of the sensor which gives velocity in mm/s (Böðvarsson et al., 1999). Applying a 19-min median filter removes spikes like earthquake signals from the time series. The east component was selected because of the orientation of the instrument relative to the eruption vents.

We visually inspect the continuous seismic data along with the measured SO_2 fluxes in order to look for a relationship between the two during different phases of the eruption.

2.3. Petrologic method

Groundmass glass and melt inclusion analyses were made from lava samples quenched on the field in a bucket of water and from airfall tephra. The data reported in this paper covers the whole eruption: the first sample was collected on March 21 and the last analyzed sample was collected on September 8, 2021.

Minerals with melt inclusions and groundmass glass were hand-picked and mounted in round 1-in. epoxy mounts (Fig. 1Sa-c). All phases were analyzed by a JEOL JXA-8230 SuperProbe electron probe micro-analyzer (EPMA) at the Institute of Earth Sciences, University of Iceland, with an accelerating voltage of 15 keV. The concentration of each element is derived from counting at the peak and the background on both sides of the peak. For glass analyses, the probe current was 10 nA and the beam diameter 10 μm. Plagioclase, pyroxene, olivine which hosted the melt inclusions were also analyzed with 10 nA and the beam was either focused or had a 5 μm diameter. For more details on the analytical procedures see (Bali et al., 2018; Halldórsson et al., 2022).

Melt inclusions were corrected for post-entrapment processes (crystallization and diffusion) following the procedure of (Caracciolo et al., 2020). Following post-entrapment correction, S-contents in melt inclusions were plotted as a function of MgO to check if the variations are consistent with fractional crystallization (Fig. 1Sd). This allowed us to discard melt inclusions which were partially affected by degassing. The most evolved undegassed melt inclusions were selected, and these had nearly identical major element compositions to the groundmass glass. The SO_2 content of the three or four most evolved undegassed melt inclusions of each sampled day were averaged to obtain the "undegassed melt" composition of that day.

The lava outgassing potential was calculated by subtracting the groundmass glass minimum from the groundmass glass average. The vent degassing potential was calculated in two ways: first, by the average (subtracting the groundmass glass average from the average evolved melt inclusion); and second, by the maximum (subtracting the groundmass glass minimum from the evolved melt inclusion maximum). We additionally calculated the total emission of SO_2 using a third approach referred to as degassed (using the sample where the groundmass glass was almost entirely degassed of S). The vent degassing potential and lava degassing potential are summed and are then multiplied by previously published volumes of lava erupted (Pedersen et al., 2022) in the corresponding time window during the eruption. We then compare the SO_2 release from this eruption calculated using the three petrological approaches and discuss the implications for utilizing petrologic estimates as an initial value for a gas dispersion forecast model in the pre-eruptive and early-eruption stages of other Icelandic volcanoes.

2.4. CALPUFF dispersion model

The CALPUFF dispersion model was used operationally during the eruption by the Icelandic Met Office to forecast on an hourly- and daily-basis where and when the SO_2 from the eruption may be present at ground-level. The emphasis was on providing the most likely location and timing of elevated SO_2 concentrations at medium to long distances from the eruption, which is where the populated areas are located (Fig. 1). Near-site forecasts were not prioritized despite the high number of daily visitors who were issued with general warnings about the potential for exposure to high concentrations of SO_2 (Barsotti et al., 2023). CALPUFF accounts for the major processes SO_2 would be expected to undergo such as physical removal processes like deposition and chemical reactions using available sunlight and precipitation (e.g. Barsotti, 2020). The model was run with 2 km spatial resolution. The average SO_2 emission rates from DOAS were used as a source term for the dispersion model in an ad hoc fashion, updated whenever a significant change in the average emission was measured. A detailed examination of one mid-distance air quality station showed that CALPUFF frequently over-predicted the presence of SO_2 at the ground-station (false positives). The four gridboxes closest to the measurement sites are used in the comparison of model runs to measurements.

In this work we made a series of experiments with CALPUFF to test if increasingly high temporal resolution of the time-evolving SO_2 flux term and/or the plume height would improve the model forecast of ground-level concentrations. We focussed the analysis on occasions when direct measurements showed that people had been exposed to elevated concentrations of this air pollutant. To assess the performance of each experimental forecast, the model results were compared with the direct measurements from the operational EAI air quality (AQ) network as has been done in (Whitty et al., 2023). Our experiments follow a similar experimental framework as (Holland et al., 2020) where changes to the SO_2 flux term were used to assess any improvements in forecasted SO_2 concentrations downwind from Kīlauea Volcano.

We selected the period 11 August 2021–17 August 2021 for the model experiments (Table 1) based on the following factors: a) elevated SO_2 concentrations at ground level were detected by the AQ stations on the Reykjanes Peninsula, in the Reykjavík capital area, and in South Iceland (variable distances and orientations from the eruption, Figs. 1 and 2), b) several SO_2 flux DOAS measurements with a wide range of values measured (Table 1S) and c) observed relationship between seismic tremor and SO_2 flux (Section 3.1).

Plume height is constrained in the CALPUFF simulations by modifying the exit vertical velocity of the SO_2 at the vent so that the simulated plume heights match the plume height observations. Vertical velocity has been found to have the dominant impact on controlling the final plume height while experiments have shown that changing the mixture temperature has only a minor effect on the final height, as such it was held constant at 1200 K. For the time window we were analyzing, we used the exit velocities that produced the simulated plume heights as seen in Fig. 3, which range from 0.05 to 18 m/s. The long straight lines in the measurement data are due to times without observations and do not necessarily reflect a time with stable plume heights. The dips in the modeled plume heights occur at night when the model often forecasts lower plume heights due to increased atmospheric stability and a lower boundary layer. Changes in the simulated plume height (orange in Fig. 3) which occur when the vertical velocity and SO_2 flux are unchanged are due to atmospheric instability.

Table 1
CALPUFF experiments.

ID	Input data	Experiment description
1	SO_2 flux and plume height used during the eruption (but with only one elevated source, i.e., the crater, with no contribution from an outgassing lava field)	can be understood to be "business as usual" as it is very similar to what was done operationally during the 2021 eruption
2	plume height used during the eruption but with time-evolving DOAS SO_2 flux updated each hour that a new DOAS measurement was acquired	an optimized version of relying on real-time flux measurements to update the model input. DOAS-based SO_2 source term is updated as new measurements come in rather than in an ad hoc manner
3	plume height used during the eruption but with the average SO_2 flux calculated using the petrological method	equivalent to using a melt-inclusion based estimate of gas flux from past eruptive activity as an a priori value prior to an eruption or prior to gas measurements or using direct measurements in an averaged way
4	plume height used during the eruption but with the SO_2 flux scaled based on the continuous time series of seismic tremor scaled to SO_2 flux	an optimized version of relying on a continuous data series. Applicable only after a relationship between tremor and SO_2 flux has been identified as being present and (for a time) unchanging
5	variable plume heights based on observations and with DOAS SO_2 flux as in (2)	the most complex source term tested; what we anticipate at the outset of these experiments would provide the best match between the forecasted concentrations compared with the station measurements
6	SO_2 flux used during the eruption but with the variable plume heights based on observations	an improvement based on plume height observations without any temporal improvement from the DOAS measurements

3. Results

3.1. Temporal changes of SO_2 flux

The full set of SO_2 flux measurements is shown in Figs. 4, 5 and Table 1S. All of the strongest SO_2 flux measurements were made by traverses. Phases 1–3b all show considerable high-temporal scale variability but are all equal within uncertainty in mean SO_2 flux: Phase 1: 48 ± 31 kg/s, Phase 2a: 40 ± 19 kg/s, Phase 2b: 55 ± 28 kg/s, and Phase 3a + 3b: 51 ± 19 kg/s. The SO_2 flux increases significantly in the middle of Phase 3c when the strongest SO_2 fluxes were measured, resulting in a mean for Phase 3c: 84 ± 50 kg/s and a large number of measurements that are outliers of the mean. Phase 4 shows a drop followed by a rise in SO_2 flux but is also distinguished by a number of very low measurements, with a mean of 82 ± 55 kg/s: equal to the mean of Phase 3c. Phase 5a is when the eruption took a one-week break. SO_2 fluxes were very weak so only two measurements were above detection limit, with a mean of 3 kg/s, too few measurements to be able to calculate a standard deviation. Phase 5b was the reawakening of the eruption after the break with an average of 85 ± 29 kg/s, again equal to Phase 3c and Phase 4.

The plume heights as assessed by two-DOAS instrument detections as well as from calibrated cameras (Barnie et al., 2023; Barsotti et al., 2023) are shown in Table 2S. The times series of the SO_2 flux plotted together with the plume height measurements is shown in Fig. 2S. There is no relationship observed between the temporal changes in SO_2 flux and plume height. It could be anticipated that greater SO_2 fluxes were measured concurrently with higher plume heights, but the data shows that the two are apparently uncoupled. A subset of the DOAS flux and the plume height measurements have been previously published in (Esse et al., 2023; Barsotti et al., 2023; Barnie et al., 2023; Scott et al., 2023).

When we examine the SO_2 flux in light of the amplitude of the concurrently measured seismic tremor, we find that there is not a very robust relationship between the two. We do see, however, through a simple visual inspection, that there is a general trend of stronger SO_2 fluxes measured concurrently with higher amplitude seismic tremor in Phases 3, 4 and 5 (Fig. 6, bottom left and bottom right) while weaker SO_2 fluxes cluster at lower amplitudes of seismic tremor. Phase 3 looks different from Phases 4 and 5, however, as there are times when there is strong emission of SO_2 concurrent with very low amplitude seismic tremor. During Phases 4 and 5, we see a more straightforward relationship of weak/strong SO_2 concurrent with low/high amplitude seismic tremor. We recognize a simple relationship in Phases 4 and 5: beneath an amplitude threshold of ≤0.2 of the seismic tremor, SO_2 emissions are very weak while above this threshold, SO_2 emissions are stronger.

Fig. 7 shows two photos from 18. May (Phase 3C) taken only 13 min apart. They show an example of different eruptive behaviors and visibly different amounts of condensation, inferred in these photos to be directly related to different strength emissions of gases and condensation nuclei, on a short time scale. Fig. 8 shows the time period that we use in the CALPUFF experiments. The tendency for low emissions of SO_2 to be concurrent with low amplitudes of seismic tremor is seen well in this time window.

The total SO_2 released over the course of each phase is shown in Table 2 and Fig. 9. For Phases 1–3, this was calculated using the phase-average fluxes and how long each phase lasted. For Phases 4 and 5, the calculation of the total SO_2 released considers the tendency for stronger SO_2 fluxes to be concurrent with higher amplitude seismic tremor. Thirty-six % of the time in Phase 4 was when the amplitude of seismic tremor was ≤0.2 (low activity). During the low activity time, the average SO_2 flux was 6 kg/s. During the 64% of the time of Phase 4 when the amplitude of seismic tremor was >0.2 (high activity), the average SO_2 flux was 90 kg/s. This leads to a calculation of the total SO_2 released during Phase 4 of 341 kt. If we had considered the average SO_2 flux measured over the entire Phase 4 to make this calculation (82 kg/s), we would have calculated 471 kt released during Phase 4. We repeat the same procedure for Phase 5b, which was at high activity for 94% of the time based on the continuous seismic tremor time series, leading to a calculated emission of 50 kt, which would have been calculated to be 53 kt if the average measured value had been applied over the entire time. We consider these calculations of total SO_2 emitted for these two phases utilizing the seismic amplitude to quantify the amount of time at high/low activity levels (and hence emission vigor levels) to be more accurate. In Phase 3, where we did not apply the seismic tremor amplitude time to the calculation of total SO_2 emitted because of the extremely poor agreement between the SO_2 flux measurements and the amplitude of seismic tremor, we can see that it is in this phase that we find the largest difference in the calculated release of SO_2 between the direct measurements and the petrological approach.

3.2. Petrological SO_2

The petrological S contents (Tables 3S and 4S) were multiplied by the volume of lava erupted during each phase provided in (Pedersen et al., 2022) (Table 2 shows the lava volumes provided by (Pedersen et al., 2022) and the resulting SO_2 emissions calculated using the petrological approach). Note that for the Degassed approach there is only the total eruption SO_2 calculated, and there is no time distinction by phases, as this approach is based on only one sample (a quenched lava sample collected on 12 April 2021 with a minimum groundmass glass of only 1 ppm S and an evolved melt inclusion maximum of 1165 ppm S).

3.3. Results from the CALPUFF experiments

The network of ground stations operated by the EAI shows elevated SO_2 at all stations at least once during the eruption (Whitty et al., 2023, Fig. 2) but the elevated concentrations are still quite small, and rarely above the limit of concern for health (350 μg/m^3 hourly-mean). In the time window analyzed in the CALPUFF experiments, August

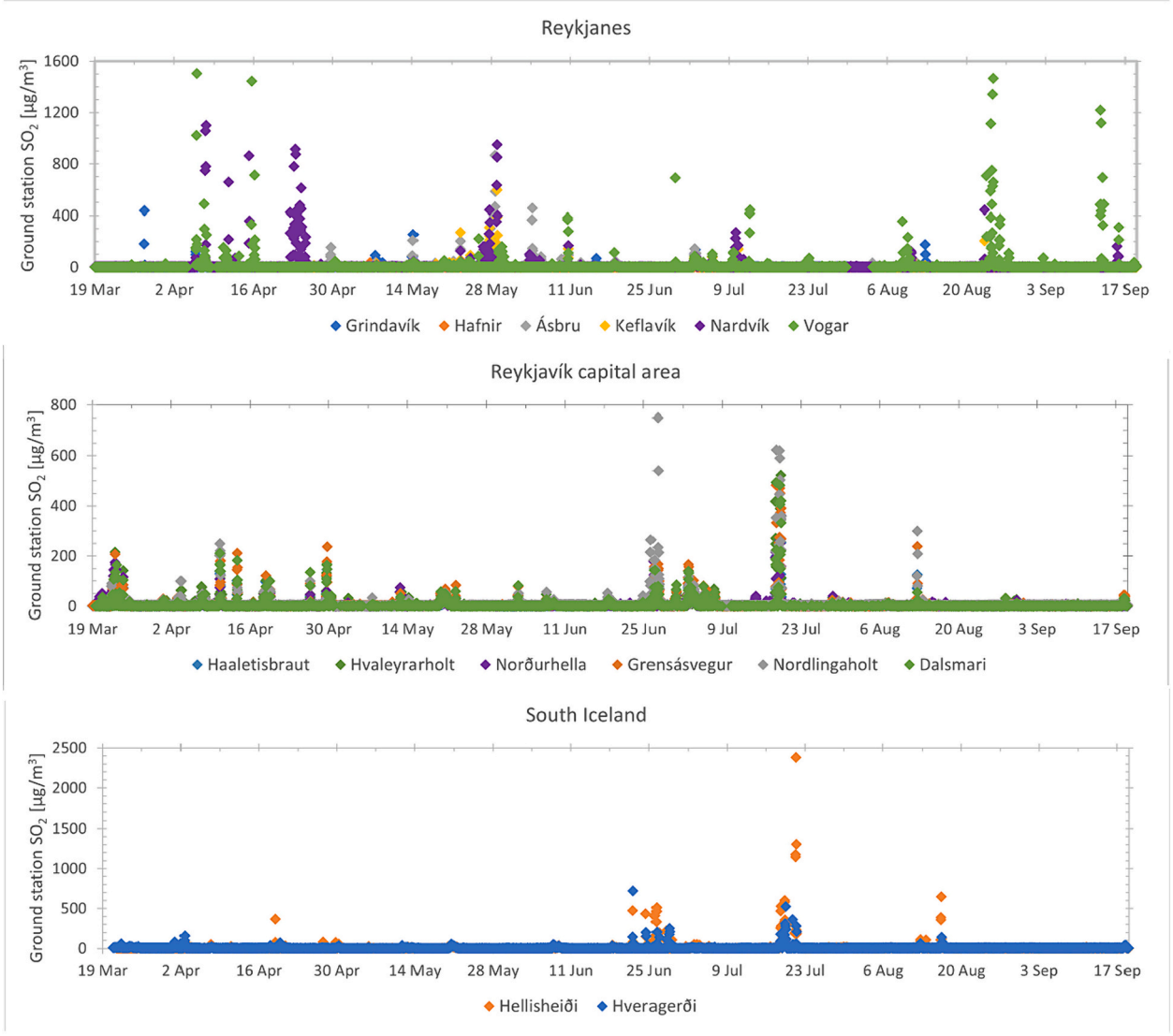

Fig. 2. SO_2 concentrations (hourly-means) measured by EAI AQ stations for the Reykjanes peninsula (top), the Reykjavík capital area (center) and South Iceland (bottom).

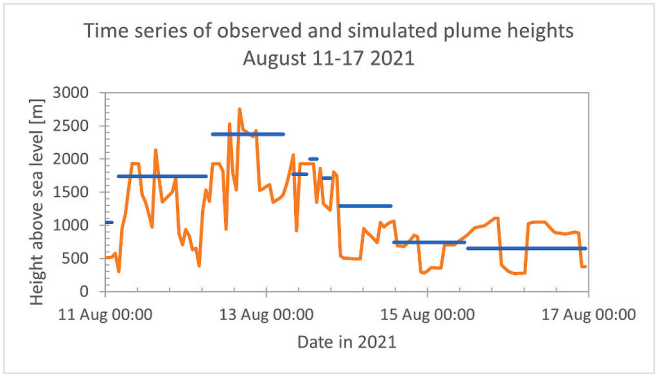

Fig. 3. Time series of observed (blue) and simulated (orange) plume heights for August 11–17 used in the CALPUFF experiments 5 and 6. (For interpretation of the references to colour in this figure legend, the reader is referred to the web version of this article.)

11–172,021, six EAI stations recorded elevations above 100 µg/m^3 SO_2 (~2 orders of magnitude above background levels): two in South Iceland (Hveragerði and Hellisheiði, ~40 km from the eruption site and ~ 10 km apart); three in the Reykjavík capital area (Norðlingaholt, Grensásvegur and Háaleitisbraut, ~30 km from the eruption and < 5 km apart) and one on the Reykjanes peninsula (Grindavík, ~10 km from eruption). The South Iceland station Hellisheiði recorded the highest concentration during the comparison period, of >600 µg/m^3; this was also the only exceedance of the air quality guideline of 350 µg/m^3 in this examined time window. In the Reykjavík capital area, the measured SO_2 concentration reached a maximum of 300 µg/m^3, i.e., slightly below the air quality guideline.

We show in Fig. 10 a time series of the station measurements and the simulation results provided by CALPUFF for the six experiments. For the Reykjanes peninsula only Grindavík is shown and for the Reykjavík capital area only Norðlingaholt as these had the highest measured concentrations in their respective regions during this time.

Run1, the "business as usual" run, forecasts the timing and concentration of the peak on the Reykjanes Peninsula (station Grindavík, Fig. 10 top left panel) well. The timing of the peaks in the capital area (station Norðlingaholt, Fig. 10 middle left panel) and in South Iceland ("He" and "Hve", Fig. 10 bottom left panel) are forecasted well, but with

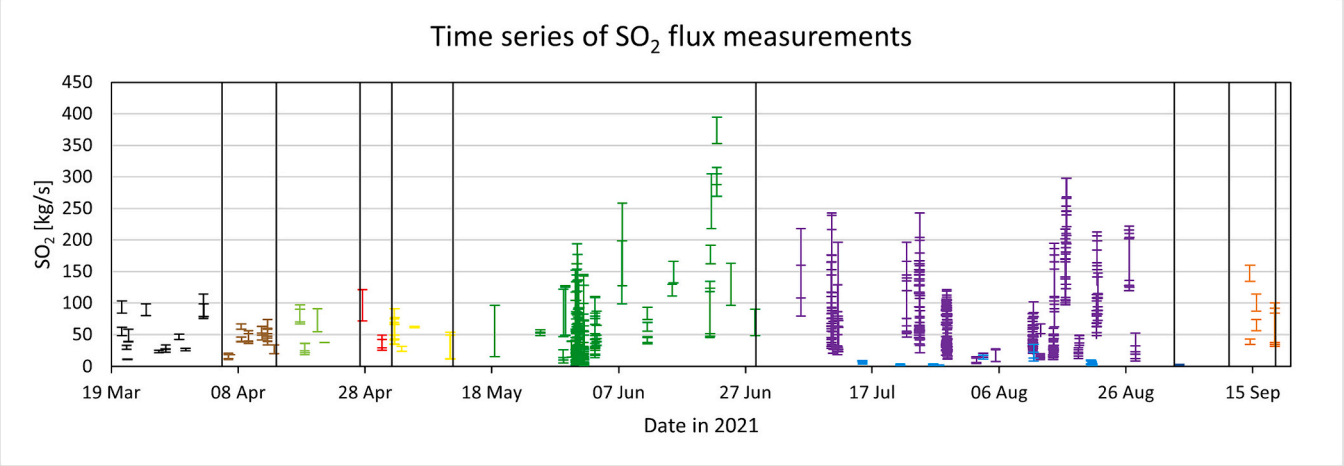

Fig. 4. Time series of SO_2 flux measured by scanning and traverse DOAS. Vertical lines indicate eruption phase transitions. Measurements made during each phase are indicated by colour: 1 (black), 2a (brown), 2b (light green), 3a (red), 3b (yellow), 3c (green), 4 (purple and light blue), 5a (dark blue), and 5b (orange). The extent of each vertical bar shows the maximum and minimum flux calculated for each traverse measurement and the uncertainty of −50% to +30% for each scan measurement. (For interpretation of the references to colour in this figure legend, the reader is referred to the web version of this article.)

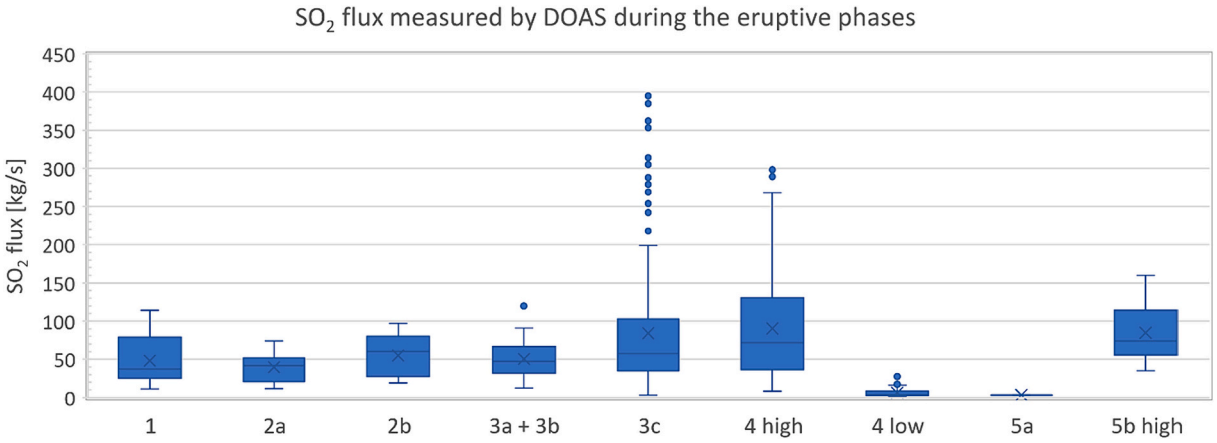

Fig. 5. A box and whisker plot of the DOAS measurements in each eruption phase.

significant underpredictions of the concentrations of these peaks. In all three regions, Run1 forecasts false positive peaks that are not detected by the EAI ground stations (Fig. 10 right panel).

Run2, based on the petrologic measurements, and Run3, based on the DOAS measurements, are essentially identical to Run1 but Run2 is often (but not always) slightly lower than Run1 while Run3 is often (but not always) slightly higher during the forecasted peaks (both peaks that are measured and those that are false positives).

Run4, applying the average SO_2 measured during high/low activity times during this phase when the seismic tremor indicates vigorous/not vigorous activity, generally provides an increase of about 1.5 to 2 times the forecasted concentrations of Run1. This is an over-prediction of the concentrations during the peak in Grindavík (which was forecasted well in Run1) and often an increase in the forecasted concentrations during the false-positives, and an improvement of the under-forecasted peak at Norðlingaholt but again with an increase in the forecasted concentrations during the false-positives. The peak at Hellisheiði remains underpredicted by the Hellisheiði Run4, but the Hveravellir Run4 forecasts the concentrations during this peak very well with the false-positive peaks again being elevated by Run4 compared with Run1.

Run5, based on the DOAS measurements and plume height measurements, is almost identical to Run1, Run2 and Run3 except at Hveravellir during the peak at Hellisheiði, where Run5 overshoots this measured peak.

Run6, based on changing only the plume height, is sometimes higher and sometimes lower than Run1. At Grindavík, Run6 improves one false positive, has no change on the most severe false positive, and overshoots the observed peak. At Norðlingaholt, Run6 worsens the false positive peak and doesn't help with the under-forecasted observed peak. The Hveragerði Run6 result matches the measurements during the Hellisheiði peak very well while not changing the concentration of the forecasted false positive.

4. Discussion

The eruption was characterized by relatively low emission rates and low plume heights although the total amount of lava makes it an average-sized Icelandic eruption (Barsotti et al., 2023; Pedersen et al., 2022). We can anticipate future eruptions on the Reykjanes peninsula in the coming years and decades or even centuries, and there have been already additional eruptions in 2022, 2023 and 2024 as of the time of this writing. For similar eruptions in the future, we recommend as best practice for the DOAS measurements that as many car traverses be made as possible, since this data is easier to process immediately following a measurement as there is more control over the measurement conditions. The scanning data requires more manual examination of the data (due to the greater amount of data coming from continuous instruments). At the same time, the scanning data is collected independently of people

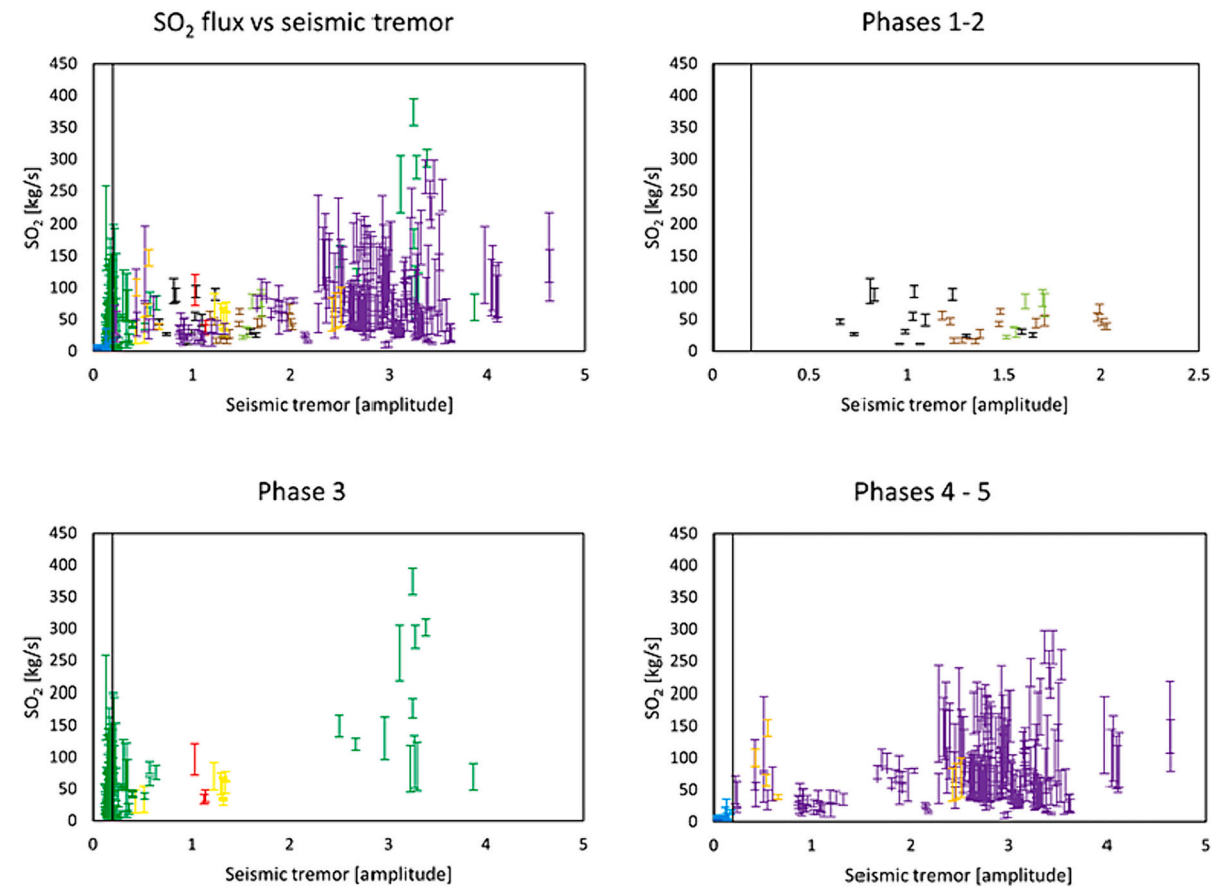

Fig. 6. SO_2 flux, colored by eruption phase as in Fig. 2, plotted against concurrent amplitude of seismic tremor. The vertical line is at an amplitude of 0.2 where a distinction is seen between low/high activity in Phases 4 and 5.

Fig. 7. Different eruptive behavior and apparent emission of gases on a short time scale. Photos taken on May 18, 2021 at 17:10 (left) and 17:23 (right) (M. A. Pfeffer).

performing a traverse, and therefore can add considerably to the number of measurements acquired during an eruption, and we recommend installing the scanners as soon as possible when deformation modeling and other geophysical parameters indicate dyke migration prior to potential eruption onset. It can be challenging to install scanning DOAS in suitable locations prior to a unrest in fissure swarms where it is not well constrained where future eruptions may occur.

For future work that will improve the SO_2 emission monitoring with DOAS, we make the following recommendations. First, the use of a supplementary scanner for wind-speed measurements using the dual-beam method (Johansson et al., 2009a) will reduce the uncertainty in wind speed. The dual-beam method employs a telescope with two off-

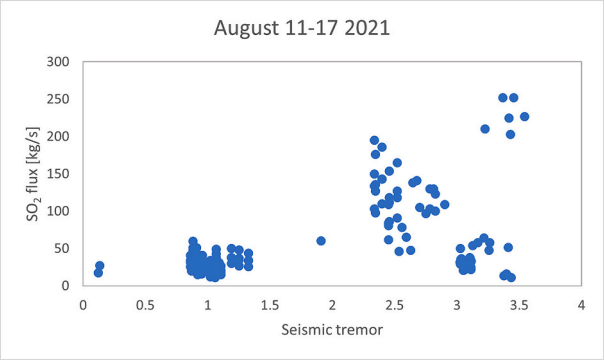

Fig. 8. A scatter plot of the SO2 flux measurements vs. the amplitude of seismic tremor measured at the same time as the DOAS measurements between August 11–172,021 (Phase 4).

axis fiber-optics couplings to a double-spectrometer, which makes possible simultaneous measurements of two plume spectra along the direction of the plume. Plume speed can be estimated by cross-correlating the time-series of column densities retrieved from the two series of measurements and estimates of the plume height. Ideally, a dual-beam instrument could be co-located with a normal scanning instrument to make parallel continuous measurements of the flux. Second, we recommend the use of plume tomography to obtain concentrations of SO_2 that could be integrated with measurements from in-situ sensors and used to work on the near-to-medium-field dispersion model predictions (Johansson et al., 2009b; Wright et al., 2008; Kazahaya et al., 2008). Our third recommendation is the routine use of scattering correction algorithm, e.g. as presented in (Galle et al., 2023) in our data processing. This is based on repeating calculations of gas using different spectral ranges and lends itself to relatively straightforward automation. We applied the scattering correction to traverse data and scan data from two days and found that the effect was minimal. This could be attributed to the low altitude of the plume, which makes dilution less probable,

Table 2
Eruption phases, volume of lava discharged from (Pedersen et al., 2022), and total emissions of SO_2 measured by the petrological calculation and DOAS as well as an assessment of if seismic tremor and SO_2 flux increase together.

Phase	Start	End	Description	Volume of lava [10^6 m^3]	Petrological calculation emission of SO_2 [kt] Average/Maximum/ *Degassed*	DOAS emission of SO_2 [kt]	Do SO_2 flux and seismic tremor increase together?
1	19.3.2021 20:40	5.4.2021 11:49	effusive eruption from one main fissure	7.0 ± 0.2	34 ± 8 / **39 ± 10**	69 ± 44	
2a	5.4.2021 11:49	14.4.2021 00:00	effusive eruption from up to 8 fissures + opening of new fissures	3.3 ± 0.3	22 ± 6 / **28 ± 7**	29 ± 14	
2b	14.4.2021 00:00	27.4.2021 05:18	effusive eruption from up to eight fissures	9.2 ± 0.8	37 ± 9 / **40 ± 10**	63 ± 32	
3a + 3b	27.4.2021 05:18	11.5.2021 21:00	lava fountains, sometimes pulsating, from one main vent	11.2 ± 1.2	83 ± 21 / **89 ± 22**	64 ± 24	
3c	11.5.2021 21:00	28.6.2021 15:00	outpouring of lava from the main crater with occasional lava fountains and persistent intra-crater activity	49.1 ± 1.5	266 ± 67 / **292 ± 73**	348 ± 204	
4	28.6.2021 15:00	2.9.2021 16:45	intermittent activity in the crater with long repose time	62.7 ± 2.4	351 ± 88 / **379 ± 95**	341 ± 203	✓
5a	2.9.2021 16:45	11.9.202 07:00	Off	0	0	2 ± 1	✓
5b	11.9.2021 07:00	18.9.2021 14:00	intermittent activity in the crater with long repose time	8.3 ± 1.7	44 ± 11 / **44 ± 11**	50 ± 17	✓
Total	19.3.2021 20:40	18.9.2021 14:00		150.8 ± 6.7	837 ± 209 / **910 ± 228** / *966 ± 242*	967 ± 538	

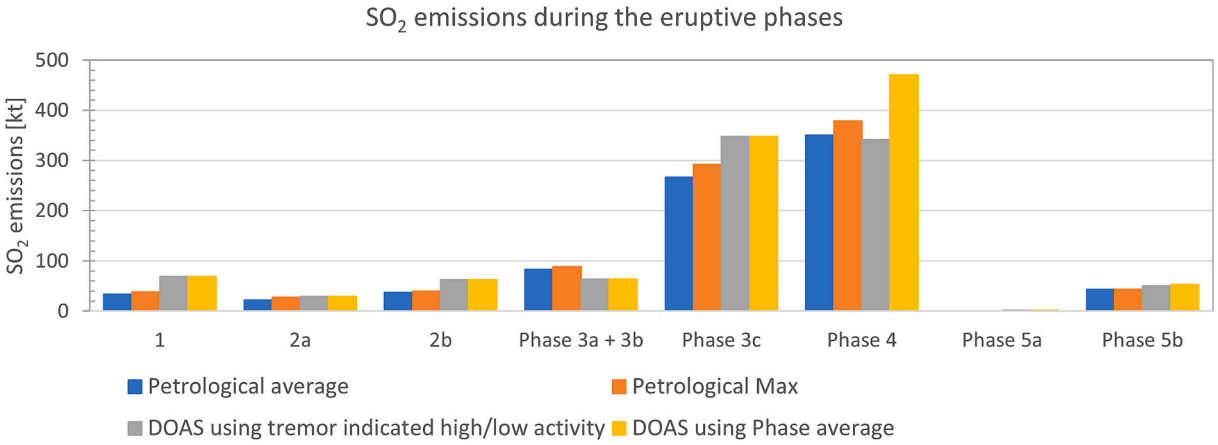

Fig. 9. The SO_2 emitted during each phase calculated by the petrological average (blue), petrological max (orange), and DOAS measurements using the seismic tremor to indicate high/low activity during phases 4 and 5 (gray) and as a phase-average without considering the in-phase differences of high/low activity (yellow). (For interpretation of the references to colour in this figure legend, the reader is referred to the web version of this article.)

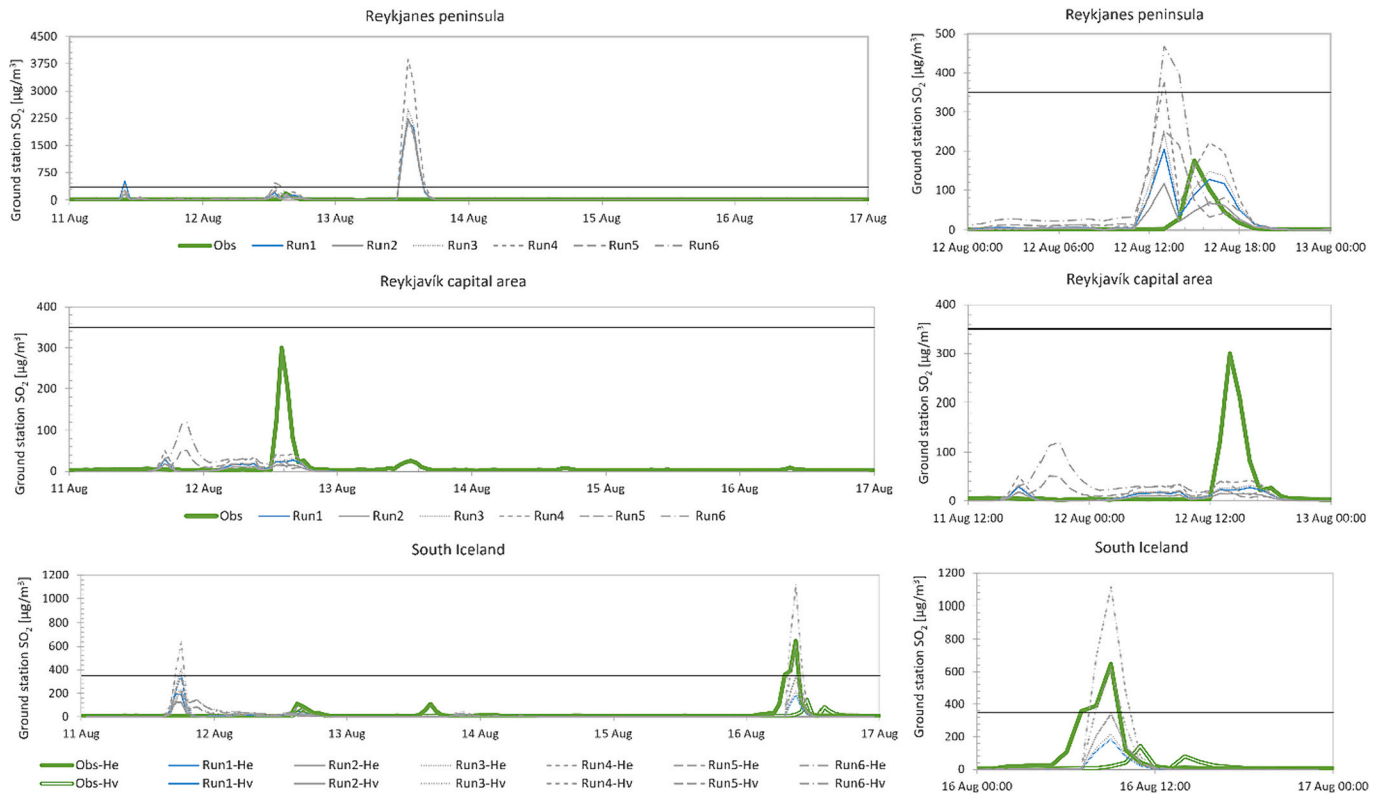

Fig. 10. Comparison of ground-level SO_2 simulated by the CALPUFF dispersion model with direct measurements by the EAI ground stations between August 11–17. Measurements of SO_2 concentrations at EAI stations are labelled "obs" (green). Grindavík is shown for the Reykjanes peninsula (top) and Norðlingaholt is shown as representative for the Reykjavík capital area (center). Hellisheiði and Hveragerði are both shown for South Iceland (bottom). Left panels show the full time period and right panels show when the hourly-mean measured SO_2 concentration exceeded 100 µg/m^3. The Iceland Directive of Health air quality guideline for hourly-mean SO_2 of 350 µg/m3 is shown as horizontal black solid lines. The model set-up most similar to that used operationally during the eruption is labelled "Run1" (blue) while Runs 2–5 are shown as shades of gray. (For interpretation of the references to colour in this figure legend, the reader is referred to the web version of this article.)

together with not having too high column densities, which limits the application of the scattering correction algorithm. We aim at implementing the correction algorithm more systematically in the real-time data processing chain, but meanwhile apply off-line checks of the data. We further recommend prioritizing automation of the post-acquisition data filtering to speed up the utilization of the scanning data.

For future work that will expand the use of the DOAS data, we recommend exploring further the correlations of SO_2 flux with seismicity when possible. As we saw in this data set, a tremor/SO_2 tendency is observed under specific conditions: when the eruption stabilized into a regular oscillatory pattern, with distinct high and low phases, while the plumbing remained temporarily unchanged. These conditions may take time to evolve in each eruption and may be present only for limited time windows. During Phase 3, we do not have a clear relationship between the SO_2 flux and the seismic tremor, as sometimes there are strong emissions of SO_2 while there is low amplitude seismic tremor. These measurements are made in late May and early June, and they coincide with the times when (Eibl et al., 2023) show in their Figure 4 that there is wind noise impacting the seismic tremor signal. Perhaps an improvement in the seismic tremor/SO_2 flux relationship can be achieved by the straightforward approach of filtering the seismic tremor time series to remove times when wind noise is having a large impact.

(Lamb et al., 2022) show that there was an increase of both acoustic and seismic activity at the onset of lava fountaining indicating activity at or near the surface. They find a second seismic tremor amplitude increase at the end of each lava fountain, when there is no concurrent acoustic increase (which might be due to a sub-surface process with no atmospheric coupling), and conclude based on their visual observations of lava fountaining and the acoustic/seismic relationship that seismic tremor may over-estimate how long lava fountaining is actively occurring. This might lead to the tremor timeseries overestimating how long SO_2 was released at elevated concentration as opposed to the low activity/low SO_2 flux times. Future refinements in ascertaining a tremor/SO_2 release relationship will be interesting, but fine details like this might have a smaller impact on the calculated SO_2 release compared with other sources of uncertainty.

Additionally, the magma composition with respect to S needs to be relatively consistent: in andesitic or rhyolitic eruptions, the S content might be more prone to change over the course of the eruption and hence the seismic tremor time series may be less predictive of the magnitude of the SO_2 emissions (Ranta et al., 2024). While the tremor/SO_2 relationship is not non-ambiguously predictive in the dataset of this eruption, we have still found that a simple application of the continuous tremor timeseries to define times of strong/weak activity has been extremely useful for calculating emissions during different eruption phases exhibiting variable activity. This simple approach works without attempting to attribute the changes in the seismic tremor due to specific causes, such as gas release directly or lava effusion. Attempting to calculate the length of strong/weak activity durations during eruptions could possibly improve the assessment of emissions from non-real-time monitored eruptions.

The "degassed" approach to calculating the amount of SO_2 emitted based on petrology provides a result consistent with that measured by DOAS. For basaltic Icelandic eruptions, in particular when the SO_2 composition of the magma is constant, using a characteristic sample with the most degassed groundmass glass might provide the best estimate of total S released during an eruption (Ranta et al., 2024), but in the absence of such a sample, the "maximum" approach is closer to the

DOAS measurements than the "average" approach.

The timing and location of elevated concentrations of SO_2 under the conditions studied here is not forecasted well by CALPUFF. The results of this model-to-observations comparison are limited, as the measured ground-level SO_2 concentrations were generally low during the analyzed time window (and the eruption as a whole had only a few peaks above health limits); the discussion here must be tempered by this limitation. All runs sometimes predict false positive elevated concentrations that were not detected by the ground stations. Some false positives are always to be expected as gases may have been transported to those places without touching the ground at that single point of the measurement station. However, false positives that occur too frequently or which are exaggerated will lead to the community distrusting the forecasts and then not taking mitigation actions when SO_2 is being accurately forecasted. Correctly predicting peaks that are experienced is considered to be the most important criteria for determining if the simulations are reliable. The default model setup does a good job predicting the closest measured peak on the Reykjanes Peninsula and the model run that utilized plume height variations improves the forecast at the furthest measured peaks in South Iceland, although with more spatial uncertainty. The mid-distance peak observed in the capital area is not predicted well by any of the runs.

The runs that improved under-predictions of observed peaks tended to increase the concentrations predicted during false positives: The result of this suite of experiments is therefore inconclusive. No approach made a significant, unambiguous improvement to the forecasted ground concentrations of SO_2, however the best model-to-observations agreement in peak SO_2 concentrations was seen closest to the eruption (Grindavík) as well as during the highest measured concentrations (South Iceland). This is an encouraging result, as forecasting accuracy becomes more important when air pollutant concentrations exceed guideline levels and when exposure frequency may be higher. In South Iceland, the forecast of SO_2 peaks was greatly improved when we treated the two measurement stations as one common area (~10 km apart). In our analysis, we always considered the forecast for the four gridboxes closest to the measurement site to be representative of the site. It might be helpful to enlarge the number of gridboxes/portion of the model domain considered to be representative for a given area as distance from the eruption, and hence spatial uncertainty, increases. The spatio-temporal uncertainties and impacts on the reliability of the forecast could be accounted for and communicated via the operational air quality advisories. For example, air quality advisories were issued on an hourly and daily basis, but perhaps daily forecasts might be more reliable such as "volcanic air pollution may be expected within the next 24 hours". With respect to the model performance with different input parameters, the operational set-up ("Run1") sometimes performed reasonably well. The improvement to the model in the highest exposure incident came from incorporating plume height observations. Based on this, we recommend prioritizing the incorporation of plume-height observations into the model runs as efficiently as possible. A promising approach for improving forecasts in the future lies in running ensemble simulations that account for uncertainties in the meteorological input as well as the eruption parameters. We leave open the possibility that the differences in the model approaches will be clearer in an eruption with higher SO_2 peaks being measured and these small peaks may simply be very difficult to forecast regardless of any attempted improvements in the modeling setup.

5. Conclusions

The 2021 eruption of Fagradalsfjall was an important opportunity to try a novel approach to linking gas and seismic monitoring data with atmospheric dispersion modeling to forecast air quality during a volcanic eruption. We investigated different approaches and concluded that incorporating real-time gas and plume height data gives promising results for improving predictions of the location and magnitude of downwind eruption-related pollution. The eruption was furthermore an excellent test case for investigating the correlation of seismic and gas emission signals under different eruption and environmental characteristics. The clearest correlation was found during modulating lava fountaining phases when there was not a big impact from wind on the seismic tremor signals. The eruption has yielded an incredibly detailed record of lava effusion rates, gas emission rates and petrological analyses. We found very consistent results between the emission of SO_2 from direct measurements and the maximum indirect reconstruction based on the petrological measurements. The SO_2 flux measurements showed a great deal of variation on short and longer time scales and during different phases of the eruption. This eruption released little SO_2 compared with previous Icelandic eruptions of the same length.

CRediT authorship contribution statement

Melissa A. Pfeffer: Writing – review & editing, Writing – original draft, Supervision, Project administration, Methodology, Investigation, Formal analysis, Data curation, Conceptualization. **Santiago Arellano:** Writing – review & editing, Software, Methodology, Formal analysis, Data curation. **Sara Barsotti:** Software, Methodology, Investigation, Funding acquisition, Formal analysis, Data curation. **Guðrún Nína Petersen:** Writing – review & editing, Methodology, Investigation, Formal analysis, Data curation. **Talfan Barnie:** Visualization, Validation, Software, Methodology, Investigation, Formal analysis, Data curation. **Evgenia Ilyinskaya:** Writing – review & editing, Visualization, Validation, Investigation, Formal analysis, Conceptualization. **Tryggvi Hjörvar:** Methodology, Formal analysis. **Enikö Bali:** Writing – review & editing, Investigation, Formal analysis, Data curation, Conceptualization. **Gro B.M. Pedersen:** Writing – review & editing, Investigation, Formal analysis, Conceptualization. **Gunnar B. Guðmundsson:** Formal analysis, Data curation. **Kristín Vogfjörð:** Formal analysis, Data curation. **Eemu Johannes Ranta:** Writing – review & editing, Formal analysis, Data curation. **Bergrún Arna Óladóttir:** Writing – review & editing, Investigation, Conceptualization. **Brock A. Edwards:** Formal analysis, Data curation, Conceptualization. **Yves Moussallam:** Writing – review & editing, Investigation, Formal analysis, Data curation. **Andri Stefánsson:** Data curation. **Samuel Warren Scott:** Data curation. **Jean-Francois Smekens:** Data curation. **Matthew Varnam:** Data curation. **Manuel Titos:** Formal analysis.

Declaration of competing interest

The authors declare they have no competing interests.

Data availability

Data will be made available on request.

Acknowledgments

Thanks to Dr. Gylfi Árnason for supplying and piloting his aircraft, TF-SRO, for the airborne SO_2 DOAS traverses. The seismic station FAF is owned by the Czech Academy of Sciences and operated in collaboration with Iceland GeoSurvey under the auspices of the NASPMOM project. The NASPMON project (NAtural Seismicity as a Prospecting and MONitoring tool for geothermal energy extraction) benefits from a € 1 370 000 grant from Iceland, Liechtenstein and Norway through the EEA Grants and the Technology Agency of the Czech Republic within the KAPPA Programme. The melt inclusion and groundmass glass analyses were supported by the Icelandic Research Fund, grant no. 228933-051. Thanks goes to Nordic EPOS for facilitating the collaboration between the Swedish and Icelandic scientists as well as to DT-GEO for paying the publication costs. Thanks for a grant (Dr. No. 149/18) from the Swedish National Space Agency to support the contributions from SA. Thank you to Dr. Kern and an anonymous reviewer for their thoughtful and helpful

comments that greatly improved the manuscript.

Appendix A. Supplementary data

Supplementary data to this article can be found online at https://doi.org/10.1016/j.jvolgeores.2024.108064.

References

Allard, P., Burton, M., Oskarsson, N., Michel, A., Polacci, M., 2011. Magmatic Gas Composition and Fluxes During the 2010 Eyjafjallajökull Explosive Eruption: Implications for Degassing Magma Volumes and Volatile Sources.

Bali, E., Hartley, M.E., Halldórsson, S.A., Gudfinnsson, G.H., Jakobsson, S., 2018. Melt inclusion constraints on volatile systematics and degassing history of the 2014–2015 Holuhraun eruption, Iceland. Contrib. Mineral. Petrol. 173 https://doi.org/10.1007/s00410-017-1434-1.

Barnie, T., Hjörvar, T., Titos, M., Sigurðsson, E.M., Pálsson, S.K., Bergsson, B., Ingvarsson, Þ., Pfeffer, M.A., Barsotti, S., Arason, Þ., Þorvaldsson, V.S., Von Löwis Of Menar, S., Oddsson, B., 2023. Volcanic plume height monitoring using calibrated web cameras at the Icelandic Meteorological Office: system overview and first application during the 2021 Fagradalsfjall eruption. J. Appl. Volcanol. 12, 4. https://doi.org/10.1186/s13617-023-00130-9.

Barsotti, S., 2020. Probabilistic hazard maps for operational use: the case of SO2 air pollution during the Holuhraun eruption (Bárðarbunga, Iceland) in 2014–2015. Bull. Volcanol. 82, 56. https://doi.org/10.1007/s00445-020-01395-3.

Barsotti, S., Parks, M.M., Pfeffer, M.A., Óladóttir, B.A., Barnie, T., Titos, M.M., Jónsdóttir, K., Pedersen, G.B.M., Hjartardóttir, Á.R., Stefansdóttir, G., Johannsson, T., Arason, Þ., Gudmundsson, M.T., Oddsson, B., Þrastarson, R.H., Ófeigsson, B.G., Vogfjörd, K., Geirsson, H., Hjörvar, T., Von Löwis, S., Petersen, G.N., Sigurðsson, E.M., 2023. The eruption in Fagradalsfjall (2021, Iceland): how the operational monitoring and the volcanic hazard assessment contributed to its safe access. Nat. Hazards 116, 3063–3092. https://doi.org/10.1007/s11069-022-05798-7.

Battaglia, J., Hidalgo, S., Bernard, B., Steele, A., Arellano, S., Acuña, K., 2019. Autopsy of an eruptive phase of Tungurahua volcano (Ecuador) through coupling of seismo-acoustic and SO2 recordings with ash characteristics. Earth Planet. Sci. Lett. 511, 223–232. https://doi.org/10.1016/j.epsl.2019.01.042.

Bengtsson, L., Andrae, U., Aspelien, T., Batrak, Y., Calvo, J., de Rooy, W., Gleeson, E., Hansen-Sass, B., Homleid, M., Hortal, M., Ivarsson, K.-I., Lenderink, G., Niemelä, S., Nielsen, K.P., Onvlee, J., Rontu, L., Samuelsson, P., Muñoz, D.S., Subias, A., Tijm, S., Toll, V., Yang, X., Køltzow, M.Ø., 2017. The HARMONIE–AROME model configuration in the ALADIN–HIRLAM NWP system. Mon. Weather Rev. 145, 1919–1935. https://doi.org/10.1175/MWR-D-16-0417.1.

Böðvarsson, R., Rögnvaldsson, S.Th., Slunga, R., Kjartansson, E., 1999. The SIL data acquisition system—at present and beyond year 2000. Phys. Earth Planet. Inter. 113, 89–101. https://doi.org/10.1016/S0031-9201(99)00032-1.

Caracciolo, A., Bali, E., Guðfinnsson, G.H., Kahl, M., Halldórsson, S.A., Hartley, M.E., Gunnarsson, H., 2020. Temporal evolution of magma and crystal mush storage conditions in the Bárðarbunga-Veiðivötn volcanic system, Iceland. Lithos 352–353, 105234. https://doi.org/10.1016/j.lithos.2019.105234.

Caracciolo, A., Bali, E., Ranta, E., Halldórsson, S., Guðfinnsson, G., 2023. Reykjanes Peninsula's historical eruptions: SO2 emissions and future hazard implications (preprint). Geochemistry. https://doi.org/10.31223/X5TX05.

De Moor, J.M., Aiuppa, A., Pacheco, J., Avard, G., Kern, C., Liuzzo, M., Martínez, M., Giudice, G., Fischer, T.P., 2016. Short-period volcanic gas precursors to phreatic eruptions: insights from Poás Volcano, Costa Rica. Earth Planet. Sci. Lett. 442, 218–227. https://doi.org/10.1016/j.epsl.2016.02.056.

Devine, J.D., Sigurdsson, H., Davis, A.N., Self, S., 1984. Estimates of sulfur and chlorine yield to the atmosphere from volcanic eruptions and potential climatic effects. J. Geophys. Res. Solid Earth 89, 6309–6325. https://doi.org/10.1029/JB089iB07p06309.

Directorate of Health, 2021. Health Risks Due to Air Pollution from Volcanic Eruptions—Guidelines for the Public, Second edition.

Donovan, A., Pfeffer, M., Barnie, T., Sawyer, G., Roberts, T., Bergsson, B., Ilyinskaya, E., Peters, N., Buisman, I., Snorrason, A., Tsanev, V., Oppenheimer, C., 2023. Insights into volcanic hazards and plume chemistry from multi-parameter observations: the eruptions of Fimmvörðuháls and Eyjafjallajökull (2010) and Holuhraun (2014–2015). Nat. Hazards 119, 463–495. https://doi.org/10.1007/s11069-023-06114-7.

Eibl, E.P.S., Thordarson, T., Höskuldsson, Á., Gudnason, E.Á., Dietrich, T., Hersir, G.P., Ágústsdóttir, T., 2023. Evolving shallow conduit revealed by tremor and vent activity observations during episodic lava fountaining of the 2021 Geldingadalir eruption, Iceland. Bull. Volcanol. 85, 10. https://doi.org/10.1007/s00445-022-01622-z.

Esse, B., Burton, M., Hayer, C., Pfeffer, M.A., Barsotti, S., Theys, N., Barnie, T., Titos, M., 2023. Satellite derived SO2 emissions from the relatively low-intensity, effusive 2021 eruption of Fagradalsfjall, Iceland. Earth Planet. Sci. Lett. 619, 118325 https://doi.org/10.1016/j.epsl.2023.118325.

Fischer, T.P., Morrissey, M.M., Marta Lucía Calvache, V., Diego Gòmez, M., Roberto Torres, C., Stix, J., Williams, S.N., 1994. Correlations between SO2 flux and long-period seismicity at Galeras volcano. Nature 368, 135–137. https://doi.org/10.1038/368135a0.

Galle, B., Oppenheimer, C., Geyer, A., McGonigle, A.J.S., Edmonds, M., Horrocks, L., 2003. A miniaturised ultraviolet spectrometer for remote sensing of SO_2 fluxes: a new tool for volcano surveillance. J. Volcanol. Geotherm. Res. 119, 241–254. https://doi.org/10.1016/S0377-0273(02)00356-6.

Galle, B., Johansson, M., Rivera, C., Zhang, Y., Kihlman, M., Kern, C., Lehmann, T., Platt, U., Arellano, S., Hidalgo, S., 2010. Network for observation of volcanic and atmospheric change (NOVAC)—a global network for volcanic gas monitoring: network layout and instrument description. J. Geophys. Res. 115 https://doi.org/10.1029/2009JD011823.

Galle, B., Arellano, S., Johansson, M., Kern, C., Pfeffer, M.A., 2023. An algorithm for correction of atmospheric scattering dilution effects in volcanic gas emission measurements using skylight differential optical absorption spectroscopy. Front. Earth Sci. 11, 1088768. https://doi.org/10.3389/feart.2023.1088768.

Halldórsson, S.A., Marshall, E.W., Caracciolo, A., Matthews, S., Bali, E., Rasmussen, M.B., Ranta, E., Robin, J.G., Guðfinnsson, G.H., Sigmarsson, O., Maclennan, J., Jackson, M.G., Whitehouse, M.J., Jeon, H., van der Meer, Q.H.A., Mibei, G.K., Kalliokoski, M.H., Repczynska, M.M., Rúnarsdóttir, R.H., Sigurðsson, G., Pfeffer, M.A., Scott, S.W., Kjartansdóttir, R., Kleine, B.I., Oppenheimer, C., Aiuppa, A., Ilyinskaya, E., Bitetto, M., Giudice, G., Stefánsson, A., 2022. Rapid shifting of a deep magmatic source at Fagradalsfjall volcano, Iceland. Nature 609, 529–534. https://doi.org/10.1038/s41586-022-04981-x.

Hidalgo, S., Battaglia, J., Arellano, S., Sierra, D., Bernard, B., Parra, R., Kelly, P., Dinger, F., Barrington, C., Samaniego, P., 2018. Evolution of the 2015 cotopaxi eruption revealed by combined geochemical & seismic observations. Geochem. Geophys. Geosyst. 19 https://doi.org/10.1029/2018GC007514.

Holland, L., Businger, S., Elias, T., Cherubini, T., 2020. Two ensemble approaches for forecasting sulfur dioxide concentrations from Kīlauea Volcano. Weather Forecast. 35, 1923–1937. https://doi.org/10.1175/WAF-D-19-0189.1.

Johansson, M., 2009. Application of Passive DOAS for Studies of Megacity Air Pollution and Volcanic Gas Emissions, Doktorsavhandlingar vid Chalmers Tekniska Högskola. Chalmers Univ. of Technology, Göteborg.

Johansson, M., Galle, B., Rivera, C., Zhang, Y., 2009a. Tomographic reconstruction of gas plumes using scanning DOAS. Bull. Volcanol. 71, 1169–1178. https://doi.org/10.1007/s00445-009-0292-8.

Johansson, M., Galle, B., Zhang, Y., Rivera, C., Chen, D., Wyser, K., 2009b. The dual-beam mini-DOAS technique—measurements of volcanic gas emission, plume height and plume speed with a single instrument. Bull. Volcanol. 71, 747–751. https://doi.org/10.1007/s00445-008-0260-8.

Kazahaya, R., Mori, T., Kazahaya, K., Hirabayashi, J., 2008. Computed tomography reconstruction of SO_2 concentration distribution in the volcanic plume of Miyakejima, Japan, by airborne traverse technique using three UV spectrometers. Geophys. Res. Lett. 35 https://doi.org/10.1029/2008GL034177, 2008GL034177.

Kern, C., Deutschmann, T., Vogel, L., Wöhrbach, M., Wagner, T., Platt, U., 2010. Radiative transfer corrections for accurate spectroscopic measurements of volcanic gas emissions. Bull. Volcanol. 72, 233–247. https://doi.org/10.1007/s00445-009-0313-7.

Kern, C., Lerner, A.H., Elias, T., Nadeau, P.A., Holland, L., Kelly, P.J., Werner, C.A., Clor, L.E., Cappos, M., 2020. Quantifying gas emissions associated with the 2018 rift eruption of Kīlauea Volcano using ground-based DOAS measurements. Bull. Volcanol. 82, 55. https://doi.org/10.1007/s00445-020-01390-8.

Lamb, O.D., Gestrich, J.E., Barnie, T.D., Jónsdóttir, K., Ducrocq, C., Shore, M.J., Lees, J. M., Lee, S.J., 2022. Acoustic observations of lava fountain activity during the 2021 Fagradalsfjall eruption, Iceland. Bull. Volcanol. 84, 96. https://doi.org/10.1007/s00445-022-01602-3.

Lerner, A.H., Wallace, P.J., Shea, T., Mourey, A.J., Kelly, P.J., Nadeau, P.A., Elias, T., Kern, C., Clor, L.E., Gansecki, C., Lee, R.L., Moore, L.R., Werner, C.A., 2021. The petrologic and degassing behavior of sulfur and other magmatic volatiles from the 2018 eruption of Kīlauea, Hawai'i: melt concentrations, magma storage depths, and magma recycling. Bull. Volcanol. 83, 43. https://doi.org/10.1007/s00445-021-01459-y.

Lopez, T., Tassi, F., Aiuppa, A., Galle, B., Rizzo, A.L., Fiebig, J., Capecchiacci, F., Giudice, G., Caliro, S., Tamburello, G., 2017. Geochemical constraints on volatile sources and subsurface conditions at Mount Martin, Mount Mageik, and Trident Volcanoes, Katmai Volcanic Cluster, Alaska. J. Volcanol. Geotherm. Res. 347, 64–81. https://doi.org/10.1016/j.jvolgeores.2017.09.001.

Nadeau, P.A., Palma, J.L., Waite, G.P., 2011. Linking volcanic tremor, degassing, and eruption dynamics via SO2. Geophys. Res. Lett. 38 https://doi.org/10.1029/2010GL045820 n/a-n/a.

Óladóttir, B.A., Pfeffer, M.A., Barsotti, S., Björnsson, B.B., Titos, M., Gupta, R., Stefánsdóttir, G., Tarquini, S., de Michieli Vitturi, M., 2023. Langtímahættumat Reykjanesskaga vestan Kleifarvatns Hrauna-, gas- og gjóskuvá Tækniskýrsla (Greinargerð No. 2023–01).

Olmos, R., Barrancos, J., Rivera, C., Barahona, F., López, D.L., Henriquez, B., Hernández, A., Benitez, E., Hernández, P.A., Pérez, N.M., Galle, B., 2008. Anomalous emissions of SO2 during the recent eruption of Santa Ana Volcano, El Salvador, Central America. In: Pérez, N.M., Gurrieri, S., King, C.-Y., Taran, Y. (Eds.), Terrestrial Fluids, Earthquakes and Volcanoes: The Hiroshi Wakita Volume II, Pageoph Topical Volumes. Birkhäuser, Basel, pp. 2489–2506. https://doi.org/10.1007/978-3-7643-8720-4_8.

Patrick, M.R., Orr, T., Sutton, A.J., Lev, E., Thelen, W., Fee, D., 2016. Shallowly driven fluctuations in lava lake outgassing (gas pistoning), Kīlauea Volcano. Earth Planet. Sci. Lett. 433, 326–338. https://doi.org/10.1016/j.epsl.2015.10.052.

Pedersen, G.B.M., Belart, J.M.C., Óskarsson, B.V., Gudmundsson, M.T., Gies, N., Högnadóttir, T., Hjartardóttir, Á.R., Pinel, V., Berthier, E., Dürig, T., Reynolds, H.I., Hamilton, C.W., Valsson, G., Einarsson, P., Ben-Yehosua, D., Gunnarsson, A., Oddsson, B., 2022. Volume, effusion rate, and lava transport during the 2021

Fagradalsfjall eruption: results from near real-time photogrammetric monitoring. Geophys. Res. Lett. 49 https://doi.org/10.1029/2021GL097125 e2021GL097125.
Pedersen, G.B.M., Pfeffer, M.A., Barsotti, S., Tarquini, S., de Michieli Vitturi, M., Óladóttir, B.A., Þrastarson, R.H., 2023. Lava flow hazard modeling during the 2021 Fagradalsfjall eruption, Iceland: applications of MrLavaLoba. Nat. Hazards Earth Syst. Sci. 23, 3147–3168. https://doi.org/10.5194/nhess-23-3147-2023.
Pfeffer, M., Bergsson, B., Barsotti, S., Stefánsdóttir, G., Galle, B., Arellano, S., Conde, V., Donovan, A., Ilyinskaya, E., Burton, M., Aiuppa, A., Whitty, R., Simmons, I., Arason, Þ., Jónasdóttir, E., Keller, N., Yeo, R., Arngrímsson, H., Jóhannsson, Þ., Butwin, M., Askew, R., Dumont, S., Von Löwis, S., Ingvarsson, Þ., La Spina, A., Thomas, H., Prata, F., Grassa, F., Giudice, G., Stefánsson, A., Marzano, F., Montopoli, M., Mereu, L., 2018. Ground-based measurements of the 2014–2015 Holuhraun volcanic cloud (Iceland). Geosciences 8, 29. https://doi.org/10.3390/geosciences8010029.
Platt, U., Stulz, J., 2008. Differential Optical Absorption Spectroscopy Principles and Applications. Spring-Verlag. https://doi.org/10.1007/978-3-540-75776-4.
Ranta, E., Halldórsson, S., Óladóttir, B.A., Pfeffer, M.A., Caracciolo, A., Bali, E., Guðfinnsson, G., Kahl, M., Barsotti, S., Karlsdóttir, S., 2024. Magmatic Controls on Volcanic Sulfur Emissions at the Iceland Hotspot.
Sæmundsson, K., Sigurgeirsson, M.Á., Friðleifsson, G.Ó., 2020. Geology and structure of the Reykjanes volcanic system, Iceland. J. Volcanol. Geotherm. Res. 391, 106501 https://doi.org/10.1016/j.jvolgeores.2018.11.022.
Salerno, G.G., Burton, M., Di Grazia, G., Caltabiano, T., Oppenheimer, C., 2018. Coupling between magmatic degassing and volcanic tremor in basaltic volcanism. Front. Earth Sci. 6, 157. https://doi.org/10.3389/feart.2018.00157.
Scott, S., Pfeffer, M., Oppenheimer, C., Bali, E., Lamb, O.D., Barnie, T., Woods, A.W., Kjartansdóttir, R., Stefánsson, A., 2023. Near-surface magma flow instability drives cyclic lava fountaining at Fagradalsfjall, Iceland. Nat. Commun. 14, 6810. https://doi.org/10.1038/s41467-023-42569-9.
Sigurgeirsson, M.Á., Sæmundsson, K., 2022. Fagradalsfjall- Also Known as Part of Krýsuvík-Tröllladyngja Volcanic System. Catalogue of Icelandic Volcanoes.
Varnam, M., Burton, M., Esse, B., Salerno, G., Kazahaya, R., Ibarra, M., 2021. Two independent light dilution corrections for the SO2 camera retrieve comparable emission rates at Masaya Volcano, Nicaragua. Remote Sens. 13, 935. https://doi.org/10.3390/rs13050935.
Whitty, R.C.W., Ilyinskaya, E., Barsotti, S., Pfeffer, M.A., Schmidt, A., Jóhannsson, Th., Gilbert, G.M., Hjörvar, T., Þrastarson, R.H., Fecht, D., Sigurðsson, E.M., Sæmundsson, G.G., 2023. Fine-Scale Fluctuations of SO2 and PM Dispersion from a Small Volcanic Eruption (Fagradalsfjall 2021) and Impact Population Exposures.
Wright, T.E., Burton, M., Pyle, D.M., Caltabiano, T., 2008. Scanning tomography of SO_2 distribution in a volcanic gas plume. Geophys. Res. Lett. 35 https://doi.org/10.1029/2008GL034640, 2008GL034640.